

Electronic Supplementary Information for

Variations in the Fuel Structure Control the Rate of the Back
and Forth Motions of a Chemically Fuelled Molecular Switch

*Chiara Biagini,^a Simone Albano,^a Rachele Caruso,^a Luigi Mandolini,^a José Augusto Berrocal^b
and Stefano Di Stefano^{a*}*

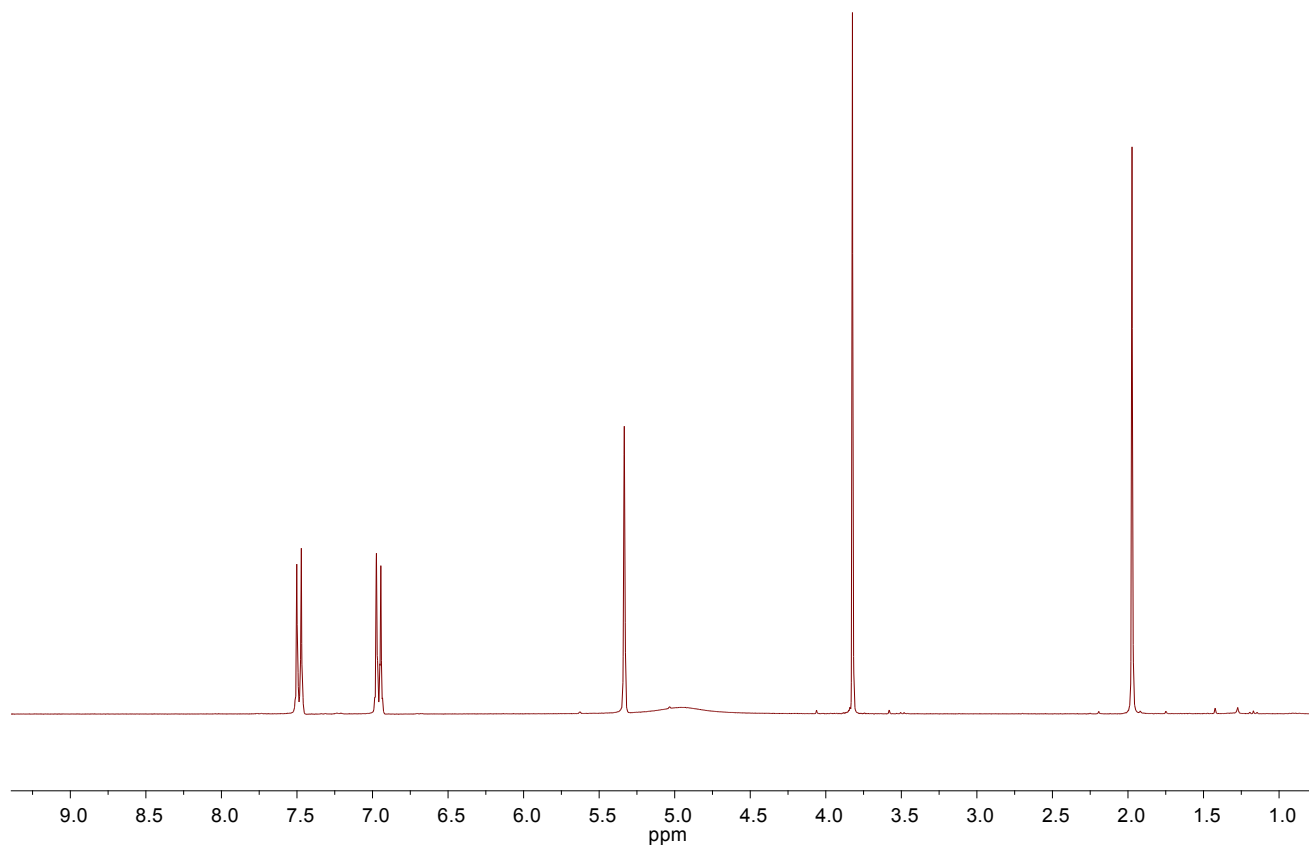
^aDipartimento di Chimica and Istituto CNR di Metodologie Chimiche-IMC, Sezione Meccanismi di Reazione c/o Dipartimento di Chimica, Università degli Studi di Roma “La Sapienza”, P.le A. Moro 5, 00185 Rome, Italy.

^bInstitute for Complex Molecular Systems, Eindhoven University of Technology, P.O. Box 513, 5600 MB Eindhoven (The Netherlands)

Contents

^1H NMR spectrum of acid 2 , X = OCH ₃	S3
^{13}C NMR spectrum of acid 2 , X = OCH ₃	S4
^1H NMR spectrum of acid 2 , X = CH ₃	S5
^{13}C NMR spectrum of acid 2 , X = CH ₃	S6
^1H NMR spectrum of acid 2 , X = Cl	S7
^1H NMR monitoring of the reaction between 2 , X = Cl and Et ₃ N	S8
^1H NMR monitoring of the reaction between 2 , X = OCH ₃ and Et ₃ N	S9
^1H NMR monitoring of the reaction between 2 , X = CH ₃ and Et ₃ N	S10
Hammett plot for reaction between 2 , X = OCH ₃ , CH ₃ , H and Cl with Et ₃ N	S11
^1H NMR monitoring of the reaction between 1 and 2 , X = Cl	S12
^1H NMR monitoring of the reaction between 1 and 2 , X = H	S13
^1H NMR monitoring of the reaction between 1 and 2 , X = CH ₃	S14
^1H NMR monitoring of the reaction between 1 and 2 , X = OCH ₃	S15
^1H NMR spectrum of $\text{1H}^+ \text{CF}_3\text{CO}_2^-$ in CD ₂ Cl ₂	S16
Consecutive first-order reactions	S17
Effect of reactant concentration	S18
Comparison of the UV-Vis spectra of B'' in the presence and absence of added salt	S19
Alternative mechanisms for reaction of 2 , X = H and 1 in the presence of Bu ₄ NBr	S20

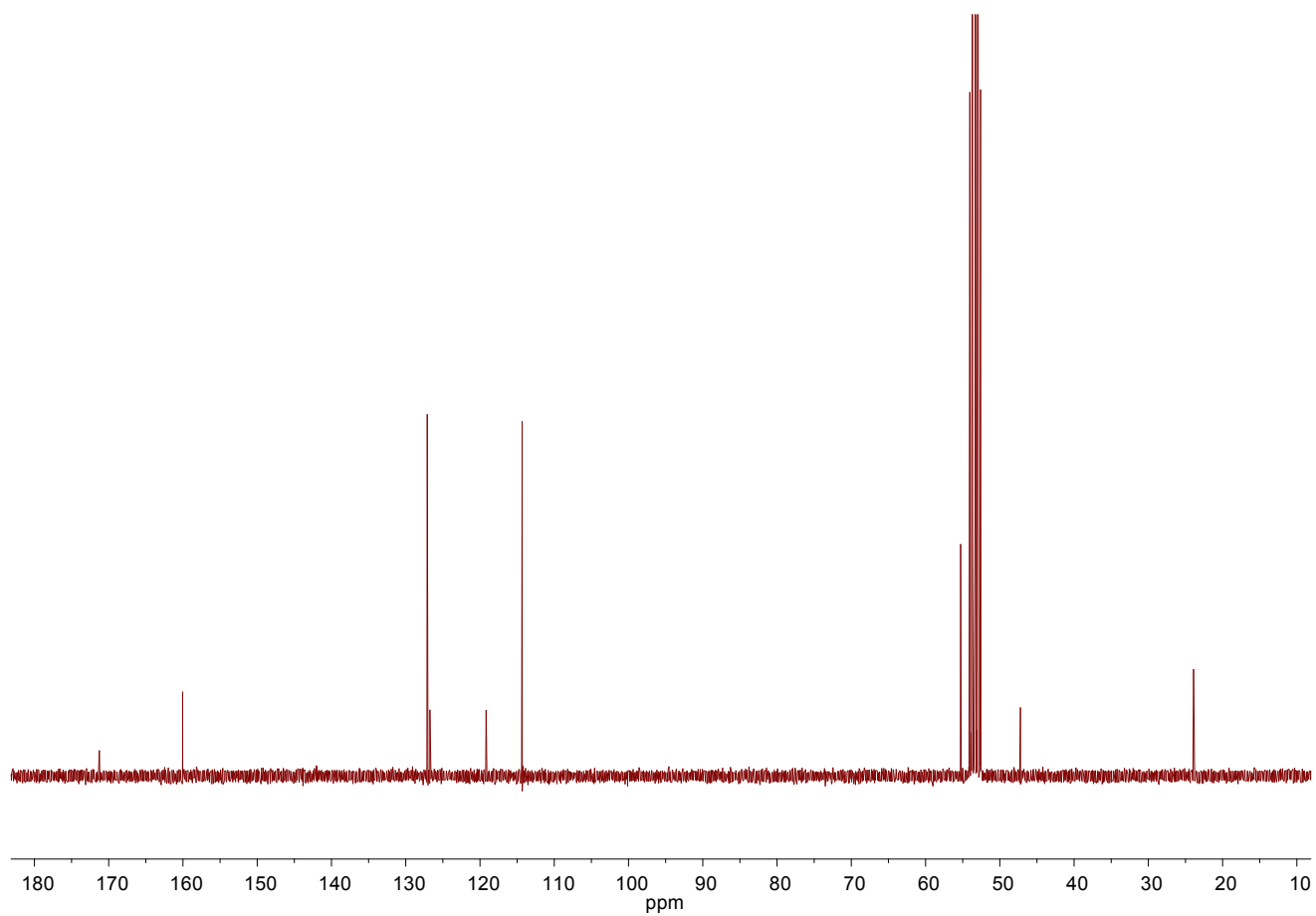
^1H NMR spectrum acid **2**, X = OCH_3



^1H NMR (300 MHz, CD_2Cl_2)

δ : 7.51-7.46 (m, 2H), 6.99-6.93 (m, 2H), 4.95 (br. s, 1H), 3.82 (s, 3H), 1.97 (s, 3H).

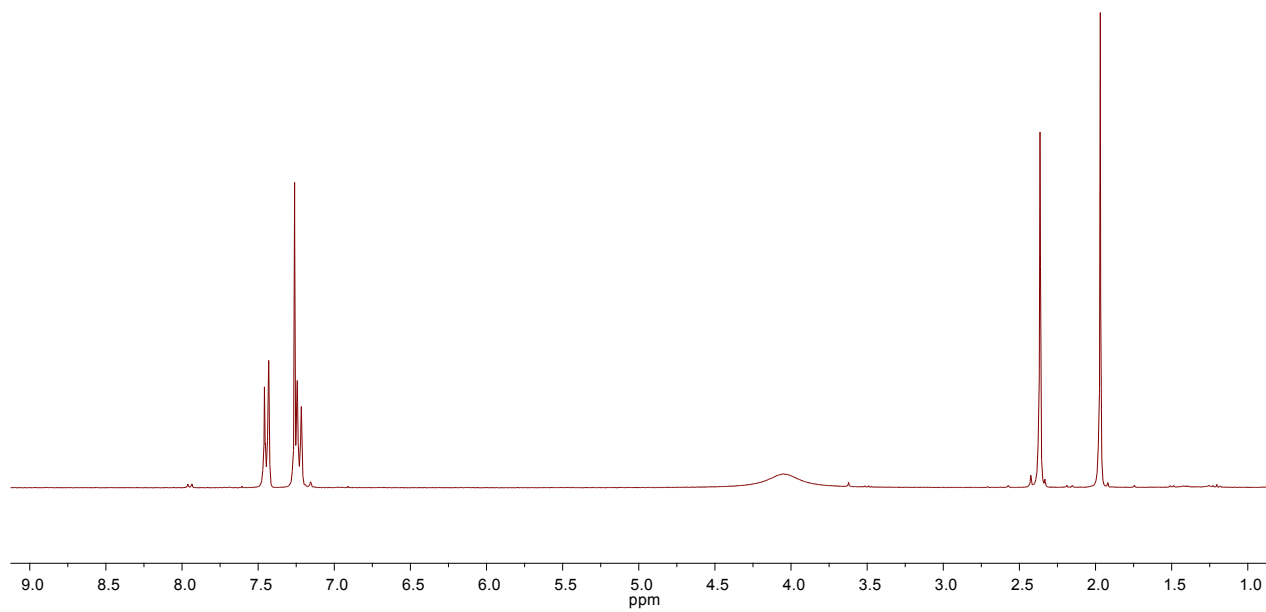
^{13}C NMR spectrum of acid **2**, X = OCH_3



^{13}C NMR (75 MHz, CD_2Cl_2)

δ : 171.3, 160.0, 127.1, 126.7, 119.2, 114.3, 55.3, 47.1, 23.8.

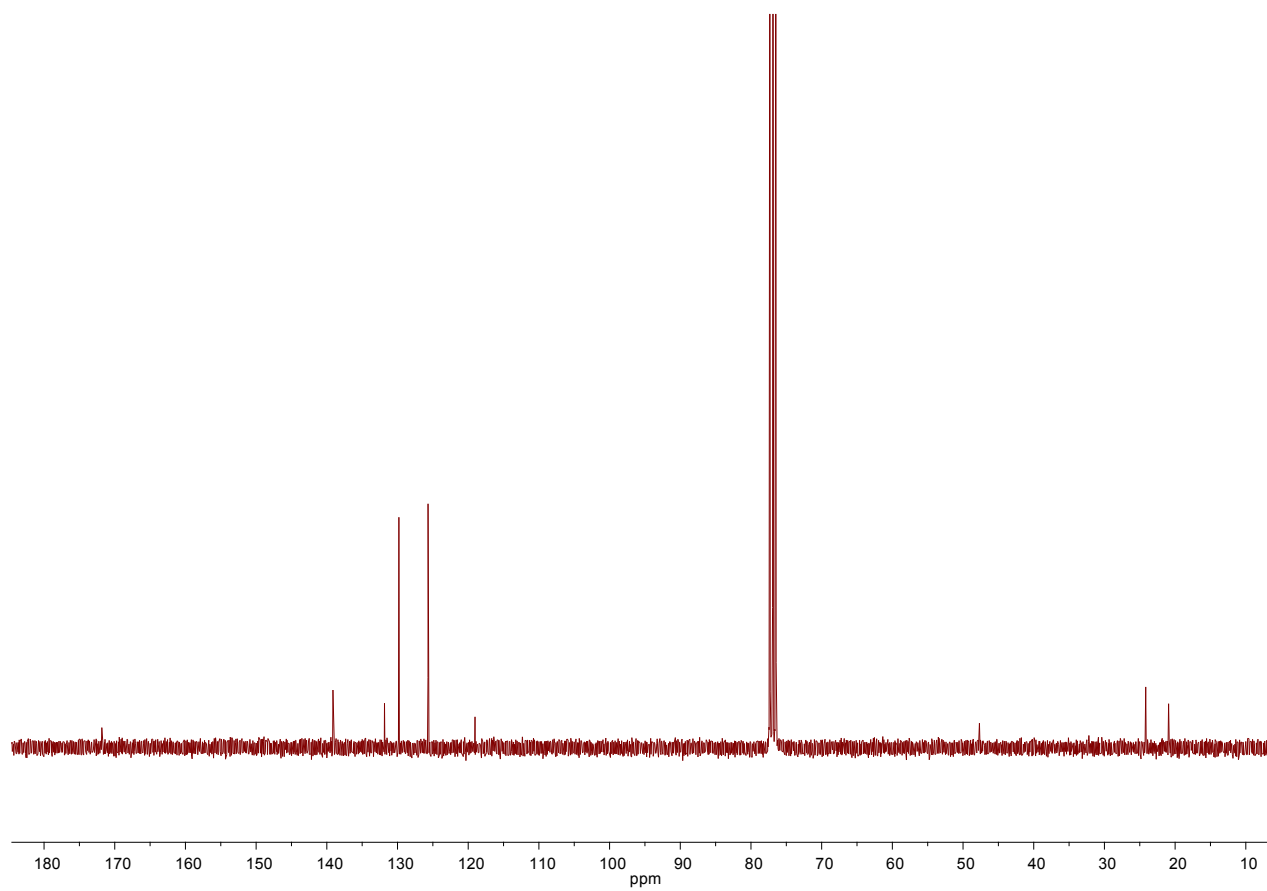
^1H NMR spectrum acid **2**, X = CH_3



^1H NMR (300 MHz, CDCl_3)

δ : 7.46-7.43 (m, 2H), 7.24-7.22 (m, 2H), 4.05 (br. s, 1H), 2.36 (s, 3H), 1.97 (s, 3H).

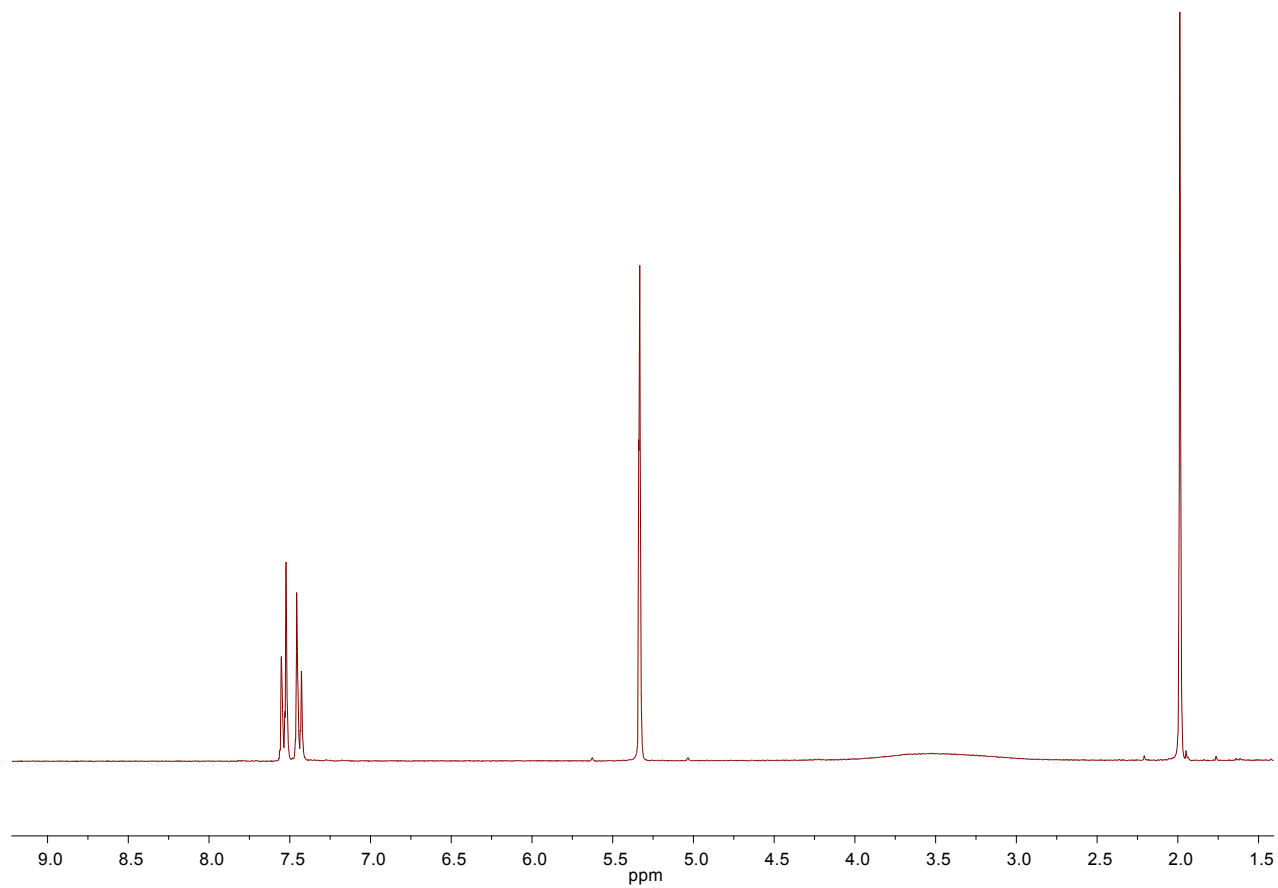
^{13}C NMR spectrum of acid **2**, X = CH_3



^{13}C NMR (75 MHz, CDCl_3)

δ : 171.2, 139.1, 131.8, 129.8, 125.7, 119.0, 47.7, 24.2, 20.9.

^1H NMR spectrum acid **2**, X = Cl



^1H NMR (300 MHz, CD_2Cl_2)

δ : 7.55–7.52 (m, 2H), 7.46–7.43 (m, 2H), 3.52 (br s, 1H), 1.99 (s, 3H).

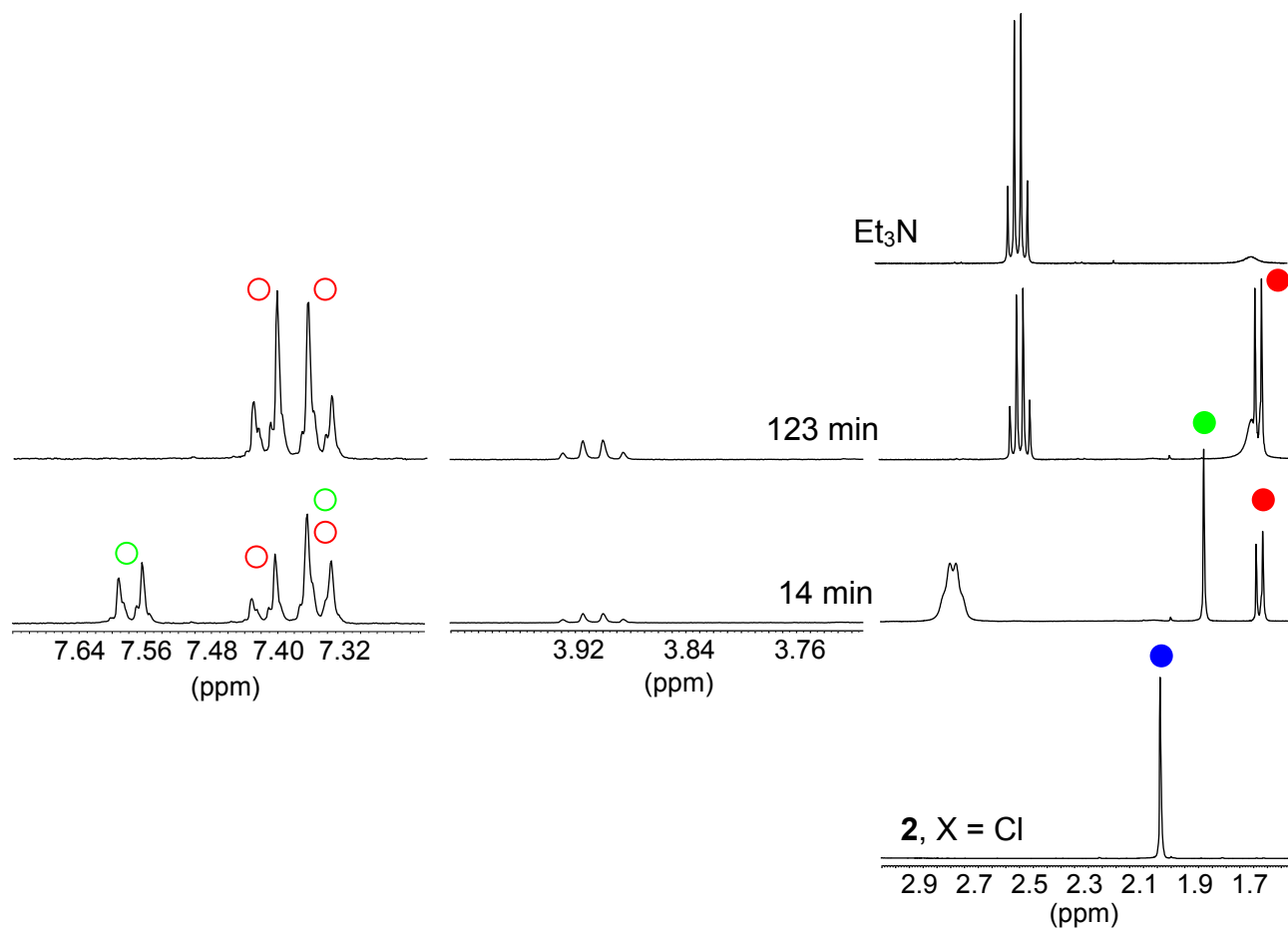
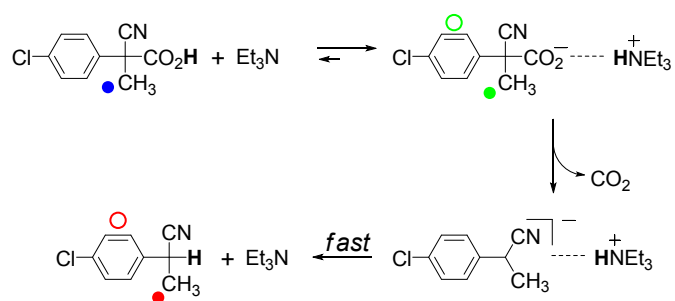


Fig. S1. Decarboxylation of 10 mM **2**, X = Cl promoted by 10 mM Et₃N in CD₂Cl₂ at 25 °C. Portion of ¹H NMR spectra recorded at $t \approx t_{1/2}$ (14 min) and $t = \infty$ (123 min). Portions of the spectra of the pure reactants are shown for comparison. The broad signal is due to adventitious H₂O.

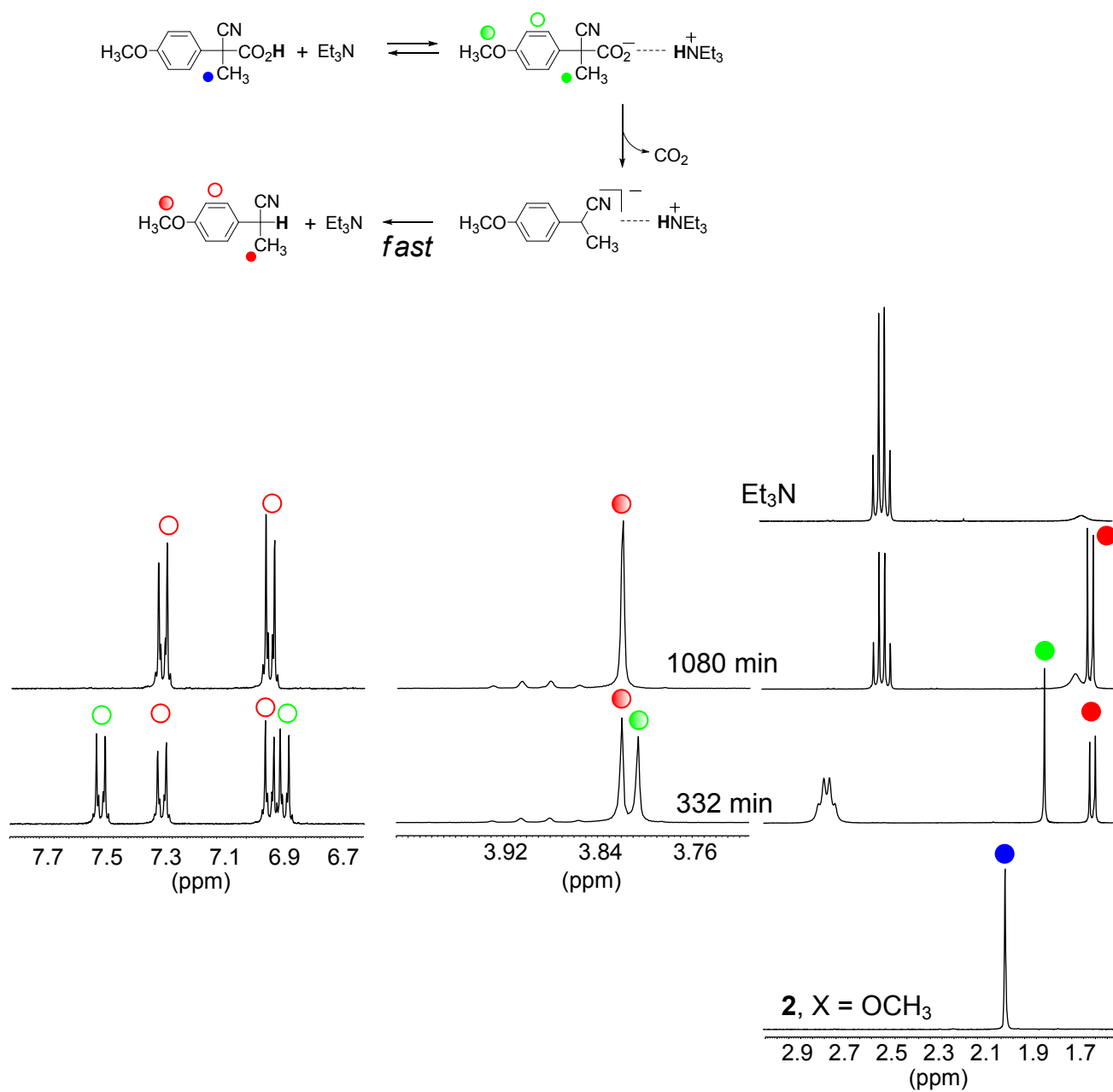


Fig. S2. Decarboxylation of 10 mM **2**, X = OCH₃ promoted by 10 mM Et₃N in CD₂Cl₂ at 25 °C. Portion of ¹H NMR spectra recorded at t ≈ t_{1/2} (332 min) and t = ∞ (1080 min). Portions of the spectra of the pure reactants are shown for comparison. The broad signal is due to adventitious H₂O.

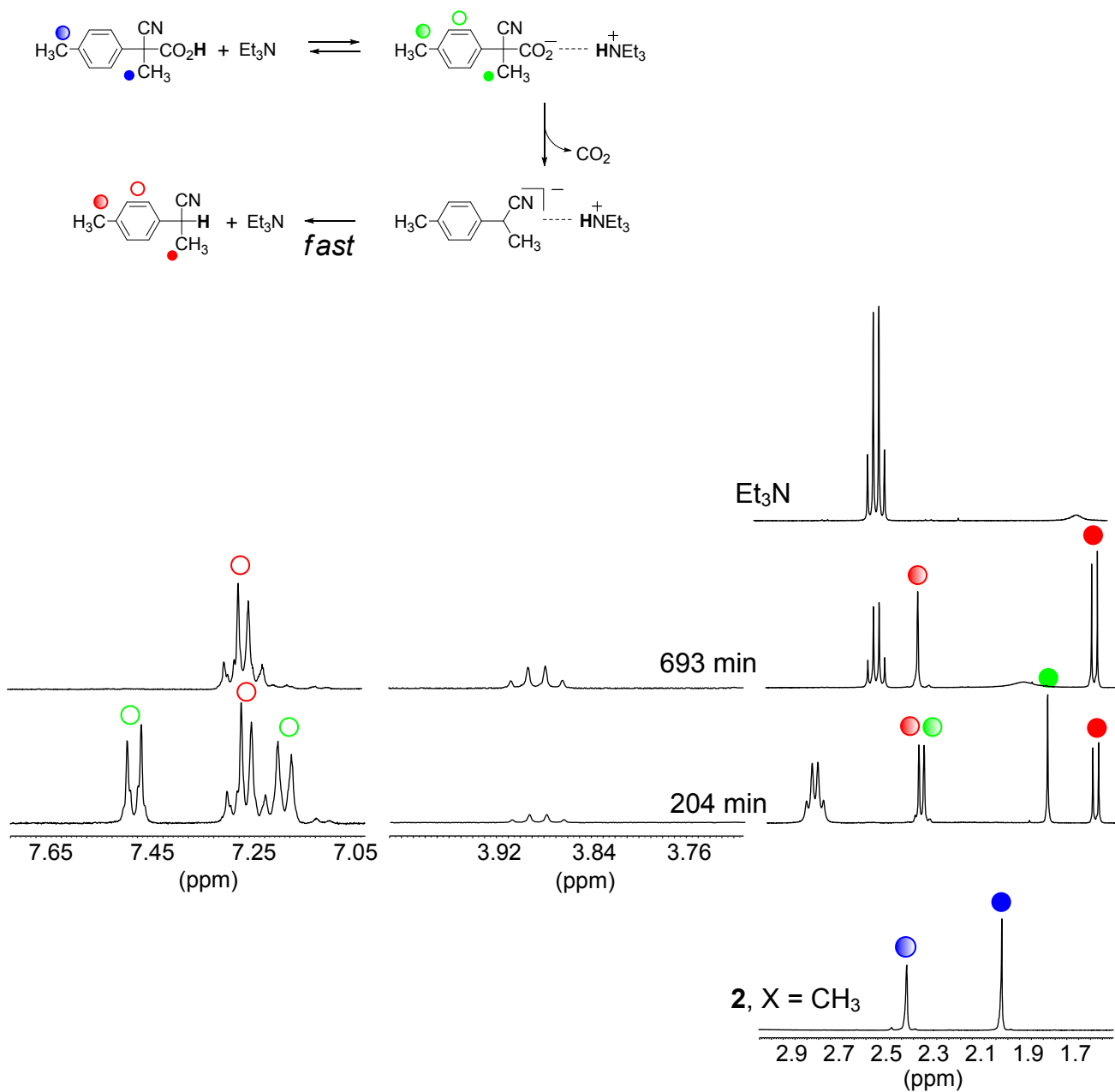
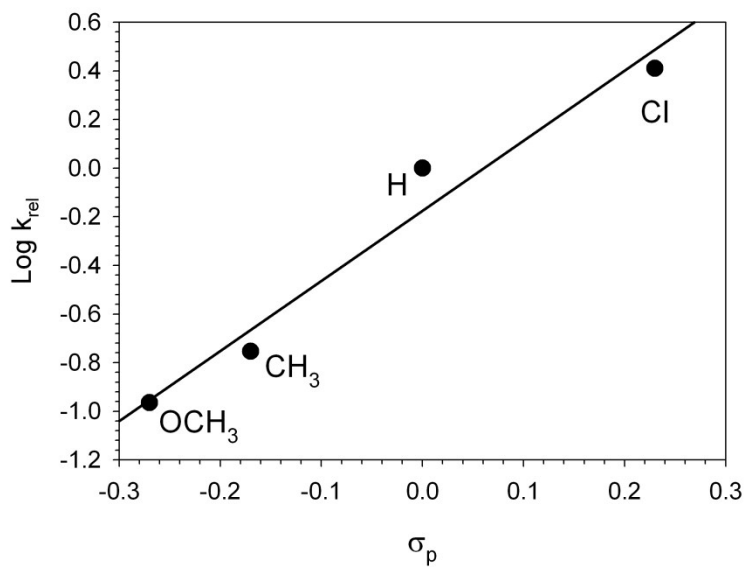


Fig. S3. Decarboxylation of 10 mM **2**, X = CH₃ promoted by 10 mM Et₃N in CD₂Cl₂ at 25 °C. Portion of ¹H NMR spectra recorded at $t \approx t_{1/2}$ (204 min) and $t = \infty$ (693 min). Portions of the spectra of the pure reactants are shown for comparison. The broad signal is due to adventitious H₂O.



$$\rho = 2.9$$

$$r = 0.9816$$

Fig. S4. Hammett plot related to reactions between 10 mM **2**, X = OCH₃, CH₃, H, and Cl with 10 mM Et₃N in CD₂Cl₂ at 25 °C.

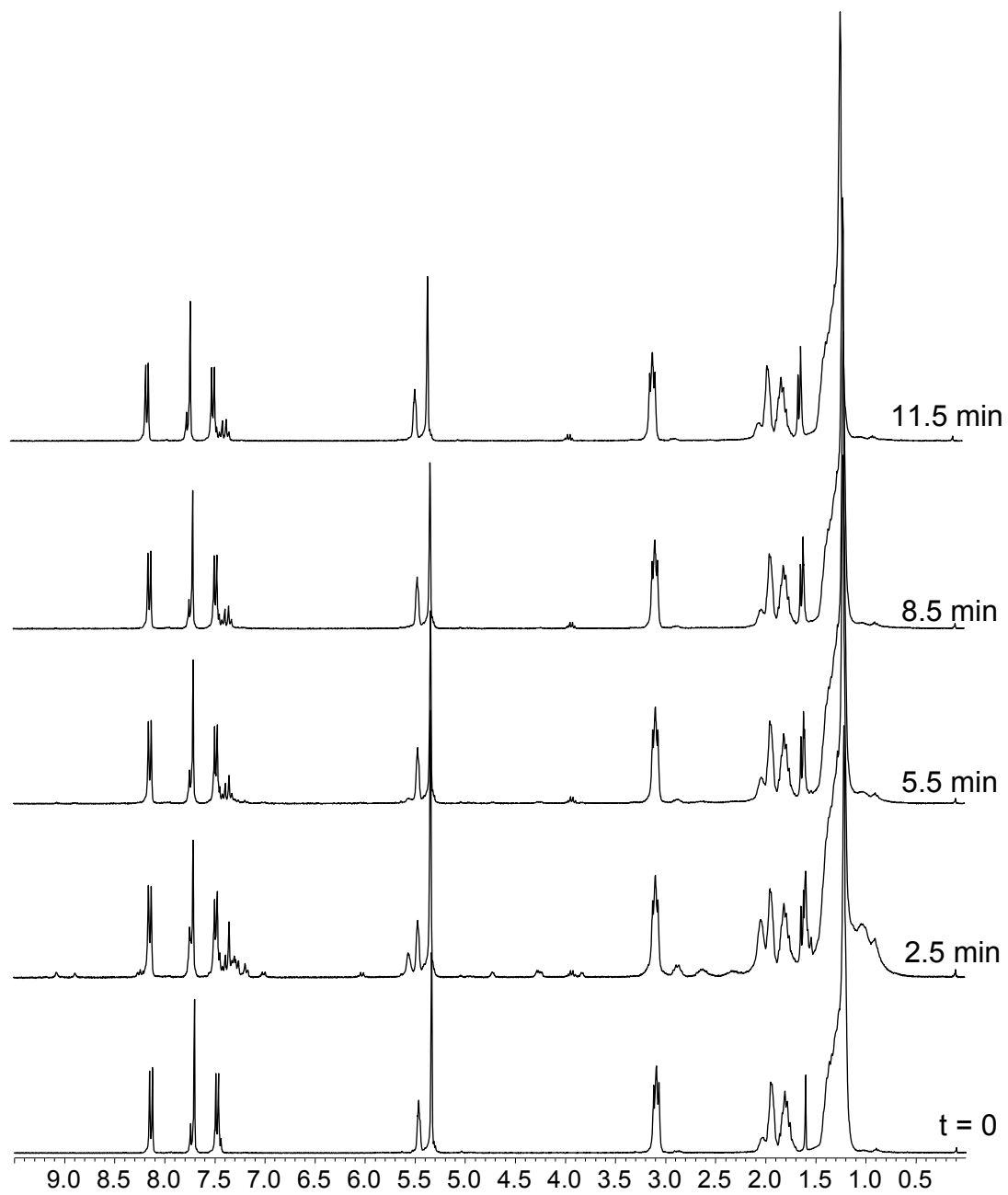


Fig. S5. ¹H NMR monitoring of the reaction between 5 mM **1** and 5 mM **2**, X = Cl in CD₂Cl₂ at 25 °C.

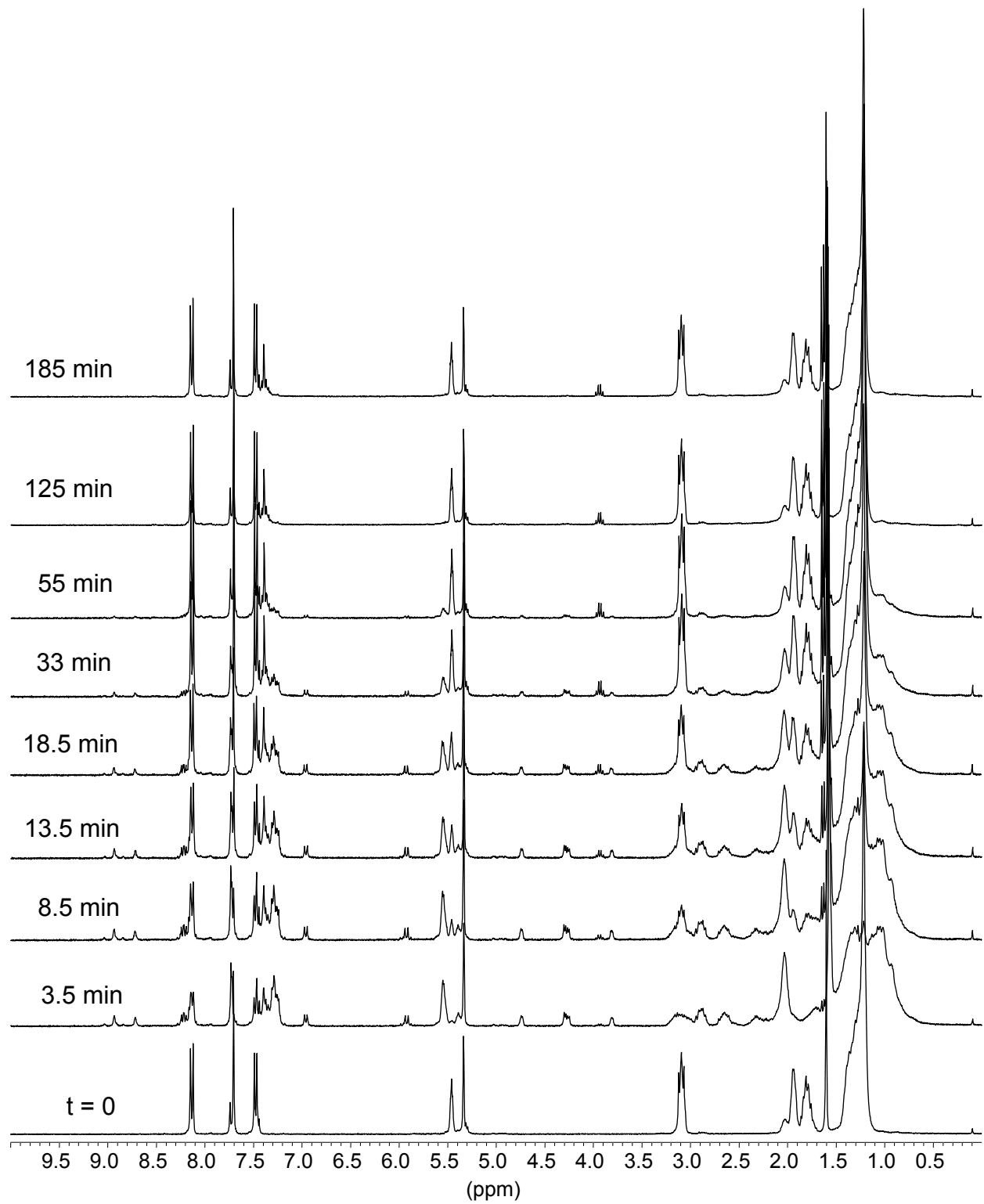


Fig. S6. ¹H NMR monitoring of the reaction between 5 mM **1** and 5 mM **2**, X = H in CD₂Cl₂ at 25 °C.

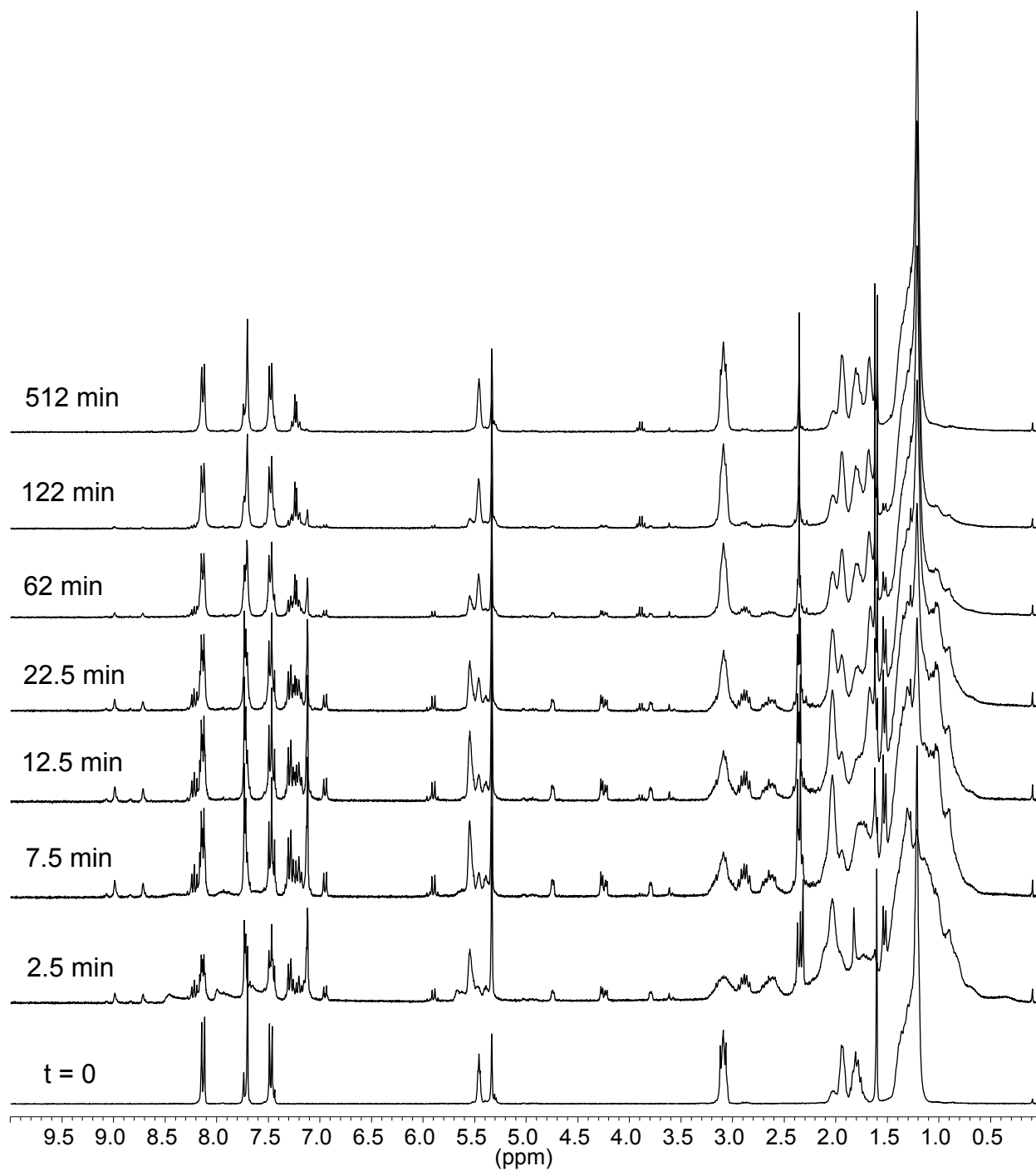


Fig. S7. ¹H NMR monitoring of the reaction between 5 mM **1** and 5 mM **2**, X = CH₃ in CD₂Cl₂ at 25 °C.

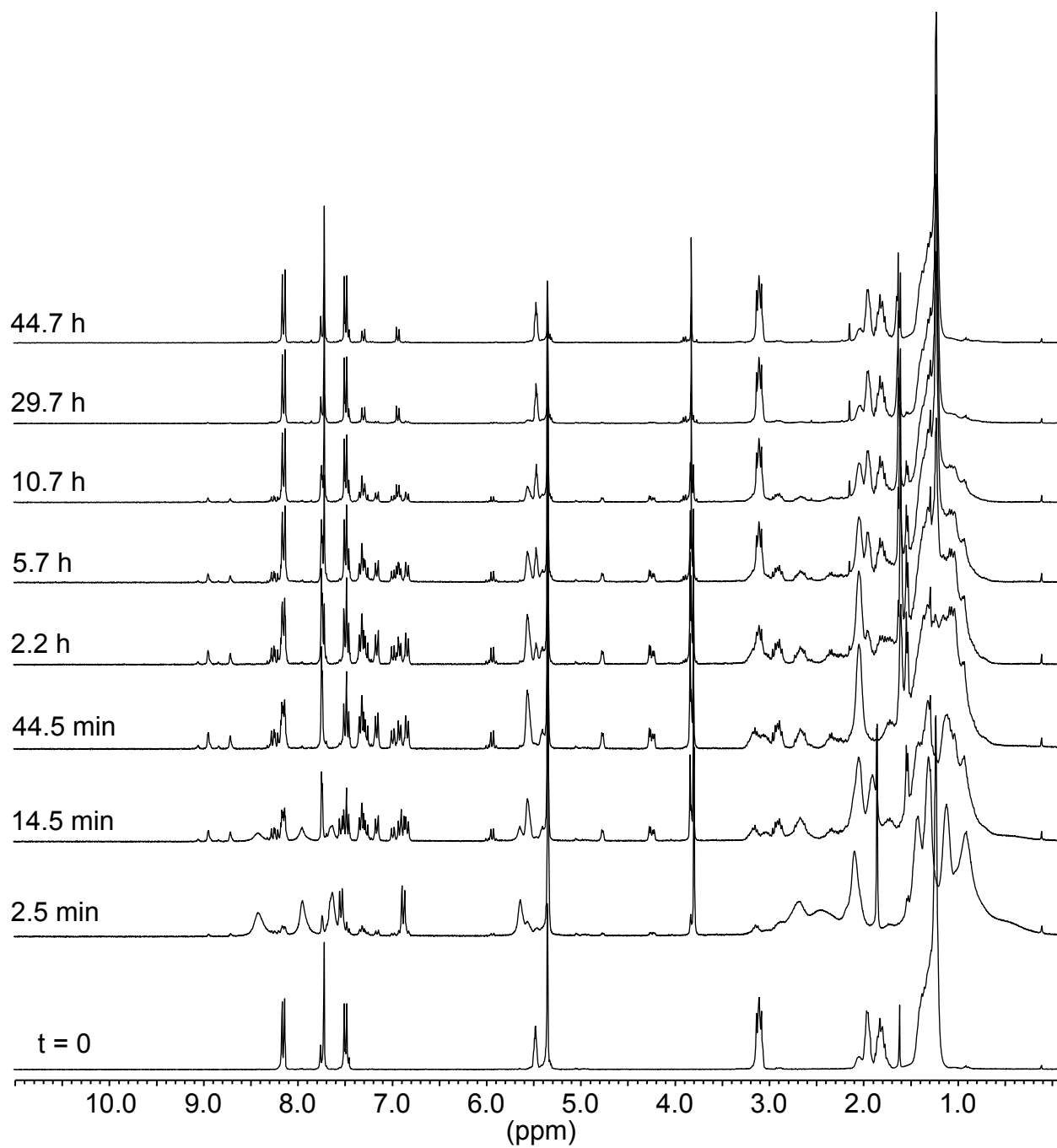


Fig. S8. ¹H NMR monitoring of the reaction between 5 mM **1** and 5 mM **2**, X = OCH₃ in CD₂Cl₂ at 25 °C.

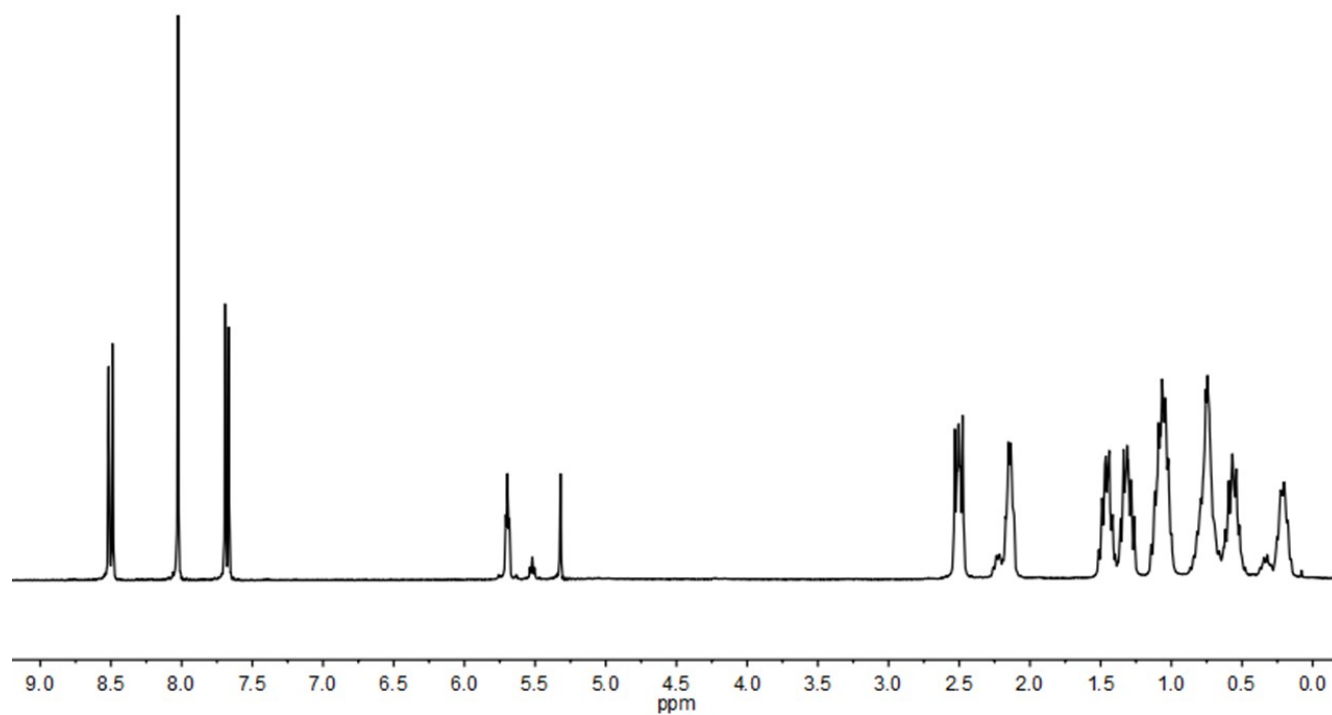
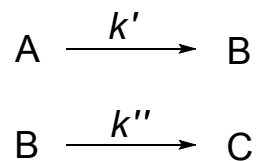


Fig. S9. ^1H NMR spectrum of $1\text{H}^+ \text{CF}_3\text{CO}_2^-$ in CD_2Cl_2 at $25\text{ }^\circ\text{C}$ (data from ref 6). Peak at 5.30 is due to CHDCl_2 .

Consecutive first-order reactions



The integrated rate eqn (S1)^{S1} reduces to the simple form of eqn (S2) when $k' \gg k''$.

$$[B] = \frac{[A]_0 k'}{k'' - k'} (e^{-k' t} - e^{-k'' t}) \quad (S1)$$

$$[B] = [A]_0 (e^{-k'' t} - e^{-k' t}) \quad (S2)$$

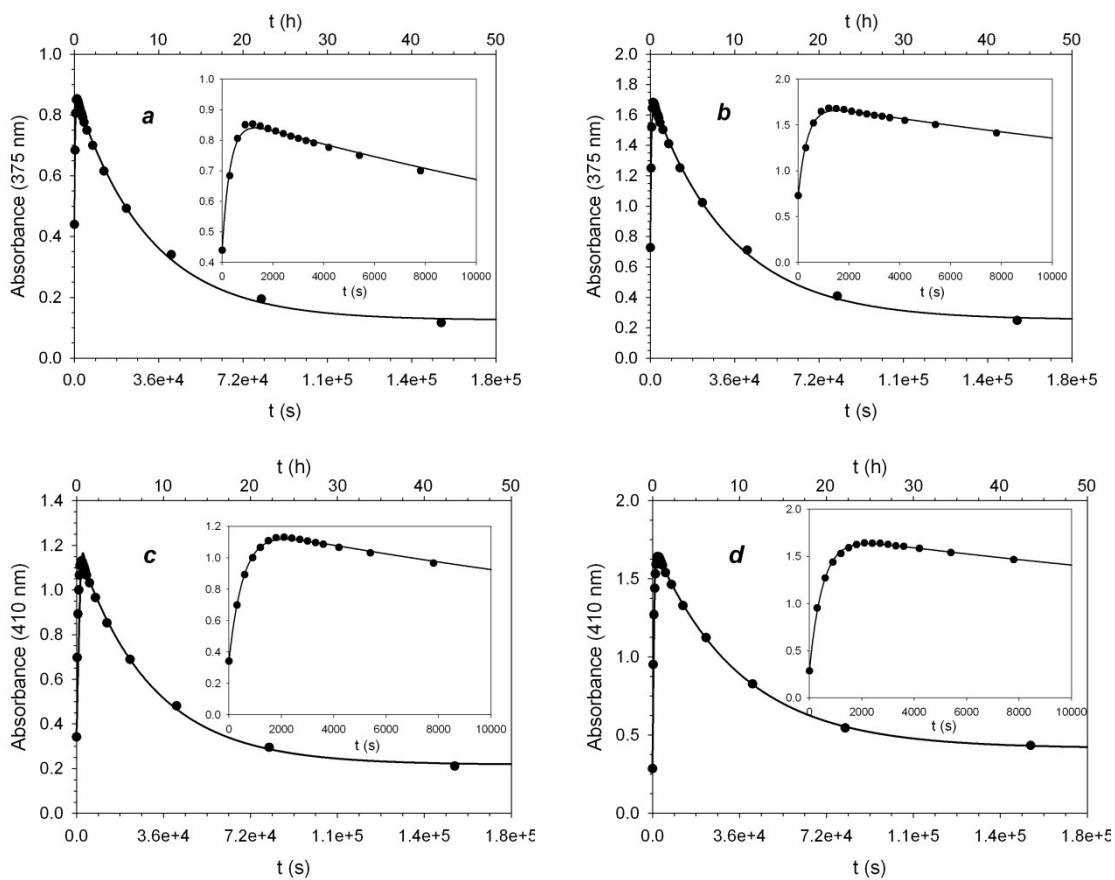
Eqn (S3) is an adaptation of eqn (S2) to the growth and subsequent decay of absorbance A in the course of the reactions of **1** with acids **2**.

$$A = A_{max} (e^{-k'' t} - e^{-k' t}) + A_0 e^{-k' t} + A_\infty (1 - e^{-k'' t}) \quad (S3)$$

A_0 and A_∞ are the absorbance values at $t = 0$ and $t = \infty$, respectively, and A_{max} is the maximum value in the absorbance-time profile.

^{S1} E. A. Frost and R. G. Pearson, Kinetics and Mechanism, 2nd Edition, John Wiley & Sons, New York 1961.

Effect of reactant concentration on the reaction of **2**, X = OCH₃ with equimolar **1** in CH₂Cl₂ at 25 °C



run	conc (mM)	$10^3 k'$ (s ⁻¹)	$10^5 k''$ (s ⁻¹)
<i>a</i>	0.30	3.2	3.2
<i>b</i>	0.60	2.8	3.0
<i>c</i>	1.00	1.9	3.3
<i>d</i>	1.50	2.0	2.8

Average

2.5 ± 0.5

3.1 ± 0.2

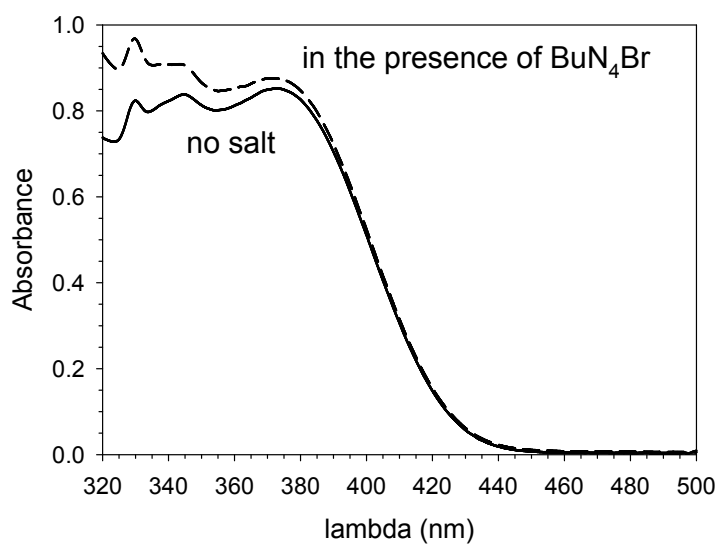
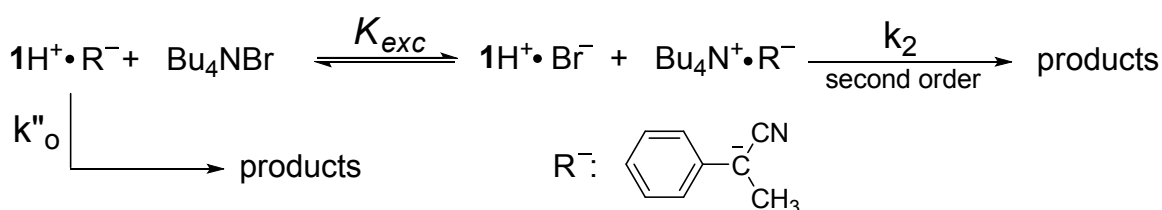


Fig. S10. Reaction between equimolar 0.30 mM **1** and **2**, X = H. Spectrum of the solution at the highest concentration of the intermediate in the absence and in the presence of 5 mM Bu₄NBr

Alternative mechanisms for reaction of 0.30 mM **2**, X = H with equimolar **1** in CH₂Cl₂ at 25 °C in the presence of increasing amounts of Bu₄NBr.

The red curve in Fig. S11 is the plot reported in the main text (Fig. 5) and is related to the association mechanism in Scheme 2

The black curve in Fig. S11 is a plot obtained from the fit of the experimental data points with the system of equations reported below, taking into account the mechanism depicted in Scheme S1. In this case, after a metathetic exchange of counterions (a sort of special salt effect), 1H⁺Br⁻ and Bu₄N⁺R⁻ react in a bimolecular fashion to give the products.



Scheme S1

$$f = k''_0 * (((C-z)/C) + k_2 * ((z^2)/C))$$

$$z = (-b - (\text{sqrt}((b^2) - 4*c*a)))/(2*a)$$

$$b = -K_{\text{exc}} * (C + x)$$

$$a = K_{\text{exc}} - 1$$

$$c = K_{\text{exc}} * C * x$$

$$k''_0 = 2.5e-4 \text{ s}^{-1}$$

fit f to y

best fit values

$$K_{\text{exc}} = 0.99 \pm 0.50$$

$$k_2 = 16.6 \pm 2.1 \text{ M}^{-1} \text{ s}^{-1}$$

$$r = 0.97$$

The system of equations reported on the left is the one used to obtain the best fit values of K_{exc} and k_2 of Scheme S1 through the calculation software Sigma Plot 10.0.

C is the concentration of reagents **1** and **2**, X = H (3×10^{-4} M);

x is the initial concentration of Bu₄N⁺Br⁻ (ranging from 0 to 5×10^{-3} M);

z is the fraction of intermediate 1H⁺ R⁻ exchanged with Bu₄N⁺Br⁻.

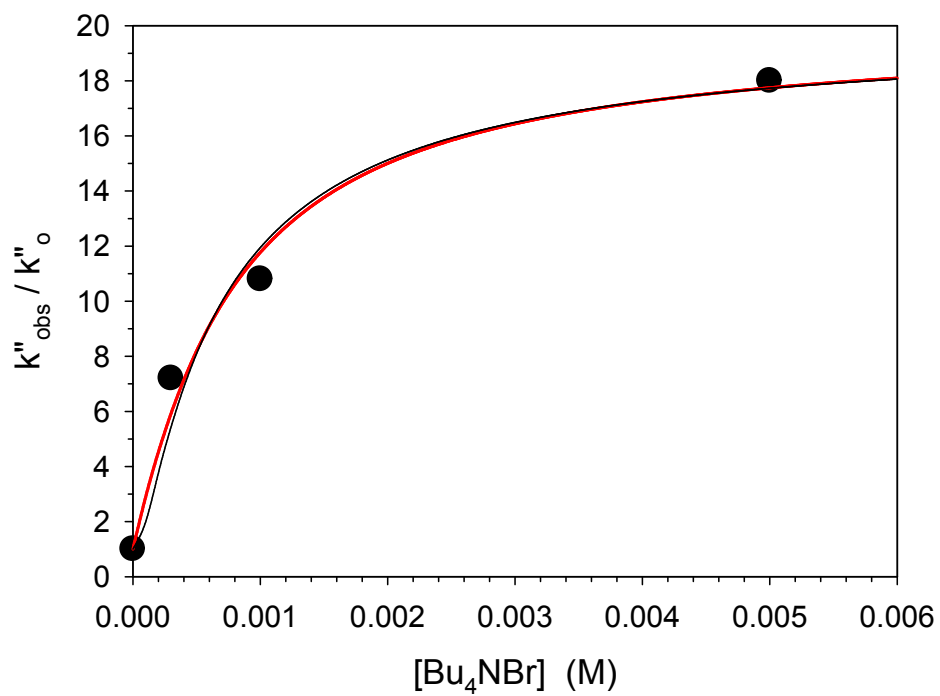


Fig. S11. Alternative fits of the data obtained for reaction of **2**, X = H with equimolar **1** in CH_2Cl_2 at 25 °C in the presence of increasing amounts of Bu_4NBr (in the case of the black fit, $k''_{\text{obs}} = k_2 \times z$).